Pergamon

Int. J. Multiphase Flow Vol. 23, No. 6, pp. 1031–1042, 1997
© 1997 Elsevier Science Ltd. All rights reserved
Printed in Great Britain

PII: S0301-9322(97)00022-0

0301-9322/97 $17.00 + 0.00

EFFECTS OF A WAVY INTERFACE ON STEAM–AIR CONDENSATION ON A VERTICAL SURFACE

S. K. PARK[1], M. H. KIM[2] and K. J. YOO[3]

[1]Korea Electric Power Research Institute, Moonji-dong 103-16, Yousoung-gu, Taejon, 305-380, Korea
[2]Department of Mechanical Engineering, POSTECH San 31, Hyoja-dong, Pohang, 790-784, Korea
[3]Korea Atomic Energy Research Institute, Daeduck Danji, P.O. Box 7, Taejon, Korea

(Received 16 October 1996; in revised form 12 March 1997)

Abstract—A correlation of vapor-side heat transfer coefficients is proposed for condensation of a steam–air mixture on a vertical surface. The correlation is based on the analogy between heat and mass transfer and includes the effects of the wavy interface between a condensate film and bulk vapor on the condensation. For a film Reynolds number less than 350, the vapor-side heat transfer coefficients are well correlated as a function of vapor Reynolds number, air–mass fraction, Prandtl number, and Schmidt number within ±10% error. The ratio of the enhanced heat transfer coefficients for the wavy interface to those with a film Reynolds number less than 350 is well correlated as a function of film Reynolds number and vapor Reynolds number within ±15% error. The film Reynolds numbers range from about 40 to 17,600 and the vapor Reynolds numbers from about 77,000 to 500,000. The air–mass fractions also range from 0.1 to 0.7. © 1997 Elsevier Science Ltd.

Key Words: film condensation, steam–air, wavy interface, vertical surface, non-condensable gas

1. INTRODUCTION

It is well known that even a small amount of non-condensable gas can reduce condensation heat transfer considerably. The reduction is mainly caused by a non-condensable gas layer formed adjacent to the condensate film (Slegers and Seban 1970; Al-Diwany and Rose 1973; Asano *et al.*, 1979; Minkowycz and Sparrow 1966; Sparrow *et al.*, 1967; Denny and Jusionis 1972; Rose 1980; Bannwart and Bontemps 1990; Hasanein *et al.*, 1996). At equilibrium the interface concentration of non-condensable gas is high enough so that the resulting diffusion and convection of this component away from the interface into the ambient just balances the rate at which its concentration increases due to the condensation. It is an additional thermal resistance exerted by non-condensable gas.

Most of the previous experimental results have shown greater heat transfer coefficients than those derived by theoretical and numerical prediction. It has been argued that an interaction between the surface waves of a condensate film and the non-condensable gas layer enhances the transport of heat and mass in the vapor mixture phase. Huhtiniemi and Corradini (1993) reported that the pendent condensate drops on a downward facing surface enhance the condensation heat transfer of a steam–air mixture. They also predicted the condensation heat transfer by using the model developed by Kim and Corradini (1990). In their model the wavy interface between condensate film and vapor phase was considered a rough wall surface. Peterson *et al.* (1993) proposed a correlation for steam condensation in the presence of non-condensable gas based on the analogy between heat and mass transfer. Their experimental data for a vertical tube were well fitted with the coefficient of 0.0276, which was greater than the 0.023 of Dittus–Boelter's correlation by about 20%. The reason was attributed to the waviness of condensate film.

Recently, some experimental results have shown that surface waves enhance the heat transfer of a steam–air mixture. Kang and Kim (1994) investigated steam–air condensation on a wavy-film

flow in a nearly horizontal rectangular duct. The condensation heat transfer increased up to several tens percents with film Reynolds number. Karapantsios *et al.* (1995) also showed that the dependence of heat transfer coefficients on the liquid flow rate was attributed to a dynamic interaction between the interfacial waves and the bulk vapor. In their experiment the steam–air mixture condensed into liquid in direct contact with subcooled water inside a vertical tube. The vapor mixture was maintained effectively stagnant. Park *et al.*(1996) examined the effects of surface waves of condensate film on steam–air condensation on a vertical surface and also analyzed the vapor-side heat transfer coefficient defined between condensate–vapor interface and bulk vapor.

This paper deals with enhanced heat transfer due to the waviness of condensate film in the diffusion layer of a steam–air mixture. The heat transfer coefficients were obtained from the three parameters of vapor velocity (U_{in} = 1.4, 3, 5, 7 m/s), air–mass fraction (W = 0.1, 0.2, 0.3, 0.5, 0.7), and film Reynolds number ($\sim$17,600) corresponding to the waviness in a vertical rectangular duct. By using the analogy between heat and mass transfer, a correlation of vapor-side heat transfer coefficients is proposed as a function of vapor-flow Reynolds number, air–mass fraction, film Reynolds number, Prandtl number, and Schmidt number. The film Reynolds number in the correlation reasonably represents the effect of the wavy interface on the enhanced vapor-side heat transfer.

2. EXPERIMENTAL FACILITIES

2.1. Experimental apparatus

The experimental facilities consisted of the test section and the auxiliary equipment; the steam–air supplying unit, the condensate-film supplying loop used to investigate the various waves of a falling-film flow, and the cooling water loop used to remove the condensation heat.

The steam flow rate was measured by an orifice flowmeter and adjusted automatically to a desired value by the feedback control valve. The air flow rate was also measured by an orifice flowmeter. The orifice flowmeters were constructed according to reference (Bean 1971). A cylindrical float flowmeter was specially used for the flow rate below 0.01 m^3/s. The accuracy was guaranteed within $\pm$ 2% error.

The description of the test section is shown in figure 1. The width and the height of the duct are 150 and 100 mm, respectively. The cooling wall was made of an aluminum alloy. The other walls were made of polycarbonate plate and insulated sufficiently. The duct and the condensing wall are 1750 and 1510 mm long, respectively. The duct was designed so that the boundary layers developed at the opposite walls did not interact. A settling chamber to enhance the quality of the steam–air flow was set up before the test duct. It consisted of a 15 mm thick honeycomb with 3 mm cells and three 20 mm screens. The temperature of the flow was measured at the inlet and the outlet of the duct.

Condensate film was circulated through the insulated closed loop and the flow rate was measured by a magnetic flowmeter. To investigate the various surface waves in a broad range of film Reynolds numbers, extra liquid was supplied at the inlet of the test duct. The supplied film was maintained nearly in a saturated state. The temperature of the liquid was measured at the inlet and the outlet to confirm whether it was equivalent to the saturated temperature.

Coolant was circulated through the closed loop to remove the condensation heat. The coolant was sufficiently supplied, so the increase of the temperature at the outlet was less than 1.5°C even at the time of maximum heat transfer rate. The size of the coolant path was 130 mm wide and 8 mm high. All temperatures were measured by calibrated T-type thermocouples and DAS (date acquisition system). Each thermocouple linked to the DAS was calibrated by a platinum resistance thermometer with a constant water bath.

2.2. Measurement of heat flux

Figure 2 shows the side and cross-sectional views of the cooling block. The size of the cooling block is 1510 mm long, 150 mm wide, and 24 mm thick. Thirty eight T-type thermocouples were installed at 2 mm inward from the upper and lower sides to measure the local heat flux. The other sides were carefully insulated to establish adiabatic condition. The dots in figure 2(a) indicate the location of the thermocouples.

The thermocouples were inserted into a copper tube with a 2 mm diameter and 45 mm long and then the copper tube was inserted into the drilled holes in the aluminum block. The junction of thermocouples was made by soldering. The wire diameter of the thermocouples was 0.254 mm. The end of the copper tube, at which the bead was soldered, had a circular cone shape. The bead was located at the apex. The gap between the drilled hole and the copper tube was filled with silver paste to reduce contact resistance.

The local heat flux was calculated from the 2-dimensional conduction equation and the proper boundary conditions which were the temperatures measured at the upper and lower sides of the block and the adiabatic condition at the other sides. The conductivity of the cooling block was precisely measured with the Ulyac TC-7000 HNC thermal conductivity meter. The heat flux measurement was checked by the direct measurement of condensate in pure steam condensation. The condensate was measured at the end of the condensing wall and compared with the calculated value from the measured heat flux and phase-change enthalpy. The direct measurement was 4.3% greater than the calculated value. The repeatability of the direct measurement of condensate was within $\pm 2\%$.

3. DATA ANALYSIS

The local film Reynolds number was calculated from the liquid film flow rate at the inlet of the test duct and the condensate on the cooling wall

$$\mathrm{Re}_f(x) = \frac{4}{\mu} m'(x) = \frac{4}{\mu} m'_{\mathrm{in}} \left[1 + \frac{1}{m'_{\mathrm{in}} h_{fv} x} \int_0^x q(x')\mathrm{d}x' \right], \qquad [1]$$

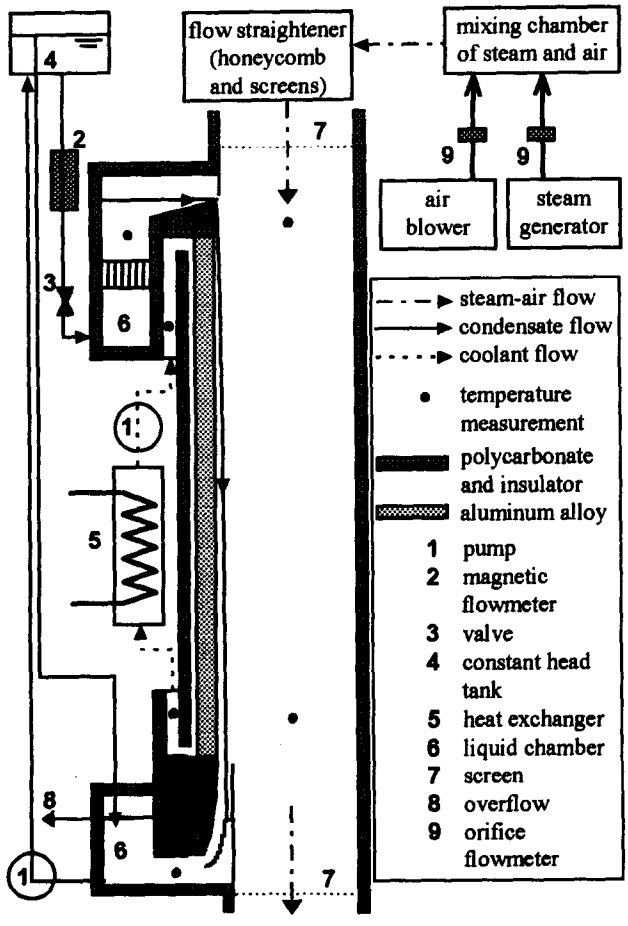

Figure 1. Side view of test section.

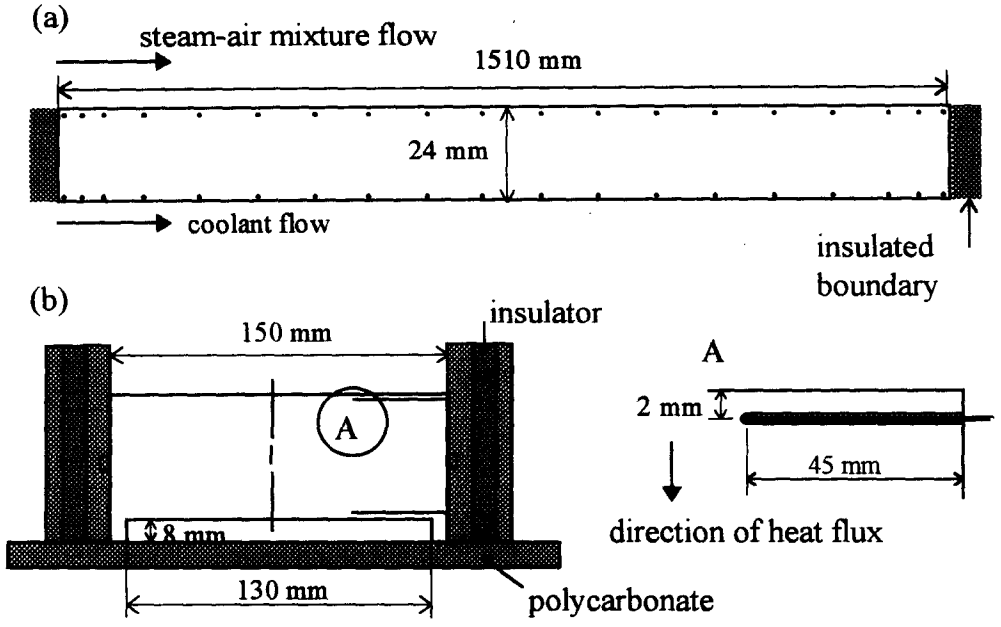

Figure 2. Configuration of thermocouples installed in the cooling block.

where $m'(x)$ is the mass flow rate per unit depth. The subscript, in, indicates the inlet of the test duct. The $q(x')$ and h_{fv} are the local heat flux and the latent heat, respectively. The μ is dynamic viscosity.

The vapor Reynolds number is defined as based on the local values

$$\mathrm{Re}_v = \frac{(U(x) - U_i)x}{v}, \qquad [2]$$

where $U(x)$ and U_i are the velocities at the core region of the test duct and at the interface respectively. The distance from the inlet of the test duct is taken for the length scale and the vapor velocity relative to the interface for the velocity scale. All transport properties of the steam–air mixture were calculated at the arithmetic mean of the bulk fluid and interface temperatures by using the method of Wilke (Reid *et al.*, 1987).

The local vapor mixture velocities along the test duct were not measured in all the experiments shown in table 1. Most of the local velocities were estimated from the inlet velocity by considering the condensation of the steam and the development of boundary layers formed on the walls. The increase of the velocity due to the development of boundary layers was about 13–16% and depended on the inlet velocity. The estimation showed good agreement with the results of some measurements in table 1 and the previous work done on the developing flow in a rectangular duct (Park 1996; Schetz 1993).

The interface velocity at the mean film thickness was calculated from the turbulent film theory developed by Yih and Liu (1983) and the laminar film theory (Nusselt 1916). The wave velocities of the condensate film

Table 1. Experimental conditions

U_{in} (m/s)	$\mathrm{Re}_{f,in}$	W	T_b(°C)†	T_w(°C)‡	U_{in} (m/s)	$\mathrm{Re}_{f,in}$	W	T_b(°C)†	T_w(°C)‡
1.4	0–15,000	0.2	95.9	70.0	3	0–13,800	0.7	76.6	49.5
1.4	0–13,700	0.3	93.4	65.8	5	0–17,200	0.1	98.1	84.1
1.4	0–12,200	0.5	86.9	58.6	5	0–16,200	0.2	95.9	76.8
3	0–12,700	0.1	98.1	78.2	5	0–15,500	0.3	93.4	75.1
3	0–16,400	0.2	95.9	78.5	5	0–12,600	0.5	86.9	60.6
3	0–14,000	0.3	93.4	66.4	5	0–14,100	0.5	86.9	69.5
3	0–15,400	0.3	93.4	75.2	5	0–12,000	0.7	76.6	58.6
3	0–12,400	0.5	86.9	58.7	7	0–17,000	0.2	95.9	81.1
3	0–13,800	0.5	86.9	68.6	7	0–15,800	0.3	93.4	76.0
3	0–15,600	0.7	76.6	58.0	7	0–14,000	0.5	86.9	68.2

†Saturation temperature of steam–air mixture in the core region of test section.
‡Mean temperature of condensing wall.

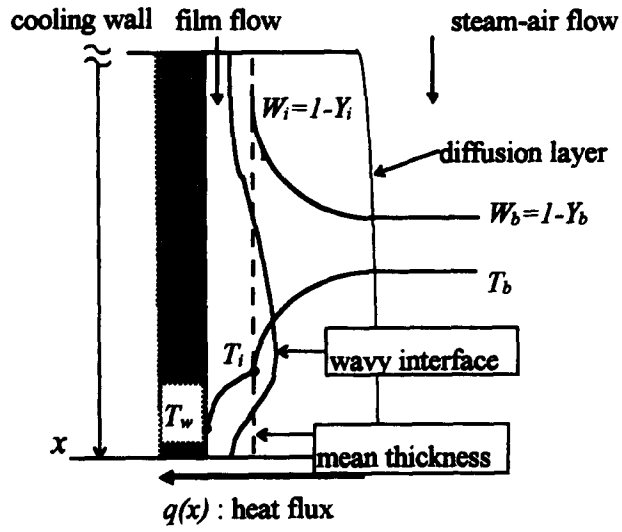

Figure 3. Diffusion layer of steam–air mixture flow.

were measured for some cases selected from among the experiments in table 1. The calculated interface velocity was reasonable when considering the propagation velocity of the waves (Park *et al.*, 1996).

From the measurements of steam and air flow rate, the air– and steam–mass fractions were calculated as follows

$$W = \frac{m_a}{m_a + m_s}; \quad Y = \frac{m_s}{m_a + m_s}. \qquad [3]$$

The air–mass fraction of the core region of the test duct always equalled that of the test duct inlet.

The main characteristic of the condensation of steam–air mixture is that the saturation temperature at the interface is lower than the bulk temperature as shown in figure 3. Three kinds of heat transfer coefficients are defined as

$$h_o = \frac{q}{T_b - T_w}; \quad h_f = \frac{q}{T_i - T_w}; \quad h_v = \frac{q}{T_b - T_i} \qquad [4]$$

where h_o, h_f, and h_v are overall, film-side, and vapor-side heat transfer coefficients. T_b and T_i are the saturation temperature at the bulk vapor and the interface. T_w is the surface temperature of the condensing wall.

There is, however, no available technique for directly measuring the interface temperature with sufficient accuracy because of the moving interface. If the film-side heat transfer coefficient is given, the interface temperature can be calculated by the following equation

$$T_i = \frac{q(x)}{h_f} + T_w. \qquad [5]$$

The following correlation obtained from the pure steam condensation was used for the film-side heat transfer coefficient (Park *et al.*, 1996)

$$\mathrm{Nu_w} = \frac{h_f(v^2/g)^{1/3}}{k} = 0.88\mathrm{Re_f}^{-0.25}, \qquad [6]$$

$$\mathrm{Nu_t} = \frac{h_f(v^2/g)^{1/3}}{k} = 0.0052\mathrm{Re_f}^{0.34}\mathrm{Pr}^{0.65}, \qquad [7]$$

where $\mathrm{Nu_w}$ and $\mathrm{Nu_t}$ are Nusselt numbers for liquid film in the case of wavy and turbulent film flow respectively.

This is based on the assumption that the film-side thermal resistance depends on the fluid properties and flow characteristic of only the condensate film regardless of the components of vapor such as pure steam or steam–air mixture. The assumption is reasonable when considering that the Nusselt number is well correlated as a function of film Reynolds number and Prandtl number, for a vertical surface, with the exception of the high interfacial shear stress. There is an argument that the surface tension and the condensing mass flux affect the wave structure of condensate film. In this experimental range of the high film Reynolds number and the

moderate vapor velocity, however, it was expected that the effect of surface tension and condensing mass flux on film-side heat transfer would be negligible as compared with that of film Reynolds number and Prandtl number (Park *et al.*, 1996).

The local heat transfer coefficients right around the entrance showed the characteristics of transition and the effect of the inlet condition, when an extra condensate film was fed. However, they disappeared in the lower part of the vertical cooling surface, as the liquid film developed thermally and hydrodynamically. Therefore, the heat transfer coefficients in the range, $x = 1.1$–1.5 m, were taken as valuable data for analysis. The local heat transfer coefficients along the cooling surface were presented and discussed in the reference (Park *et al.*, 1996).

4. RESULTS AND DISCUSSION

Figure 4 shows the vapor-side heat transfer coefficients. The horizontal axis is the vapor velocity relative to the moving interface. The velocity of the moving interface (U_i) was calculated from the turbulent film theory by Yih and Liu (1983). The arrows indicate the increase of film Reynolds number. The film Reynolds numbers corresponding to the data are also presented in the figure. The velocity of condensate film is not negligible for high film Reynolds numbers as compared with the vapor velocity. The relative velocity decreases with the increase of film Reynolds number because of the increase of the interface velocity.

In spite of the data scattering, one can find the trend that the vapor-side heat transfer coefficient increases uniquely with the increase of film Reynolds number. It is supposed that the waviness of condensate film corresponding to the film Reynolds number enhances the heat and mass transfer at the non-condensable gas layer.

4.1. *Development of correlation*

The heat flux of steam–air condensation in the saturation state is separated into condensing and sensible heat fluxes

$$q'' = q_c'' + q_s'' = -m''h_{fv}|_i + k_s\frac{\partial T}{\partial y}|_i. \qquad [8]$$

Two kinds of heat transfer coefficients corresponding to the heat fluxes are given by

$$h_c = \frac{-m''h_{fv}|_i}{T_b - T_i}, \qquad [9]$$

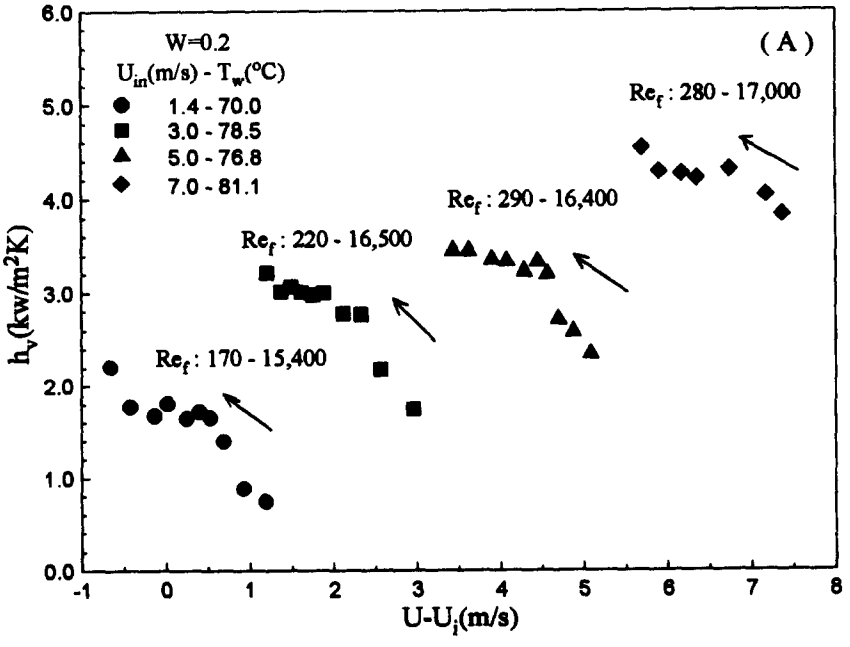

Fig. 4(a).

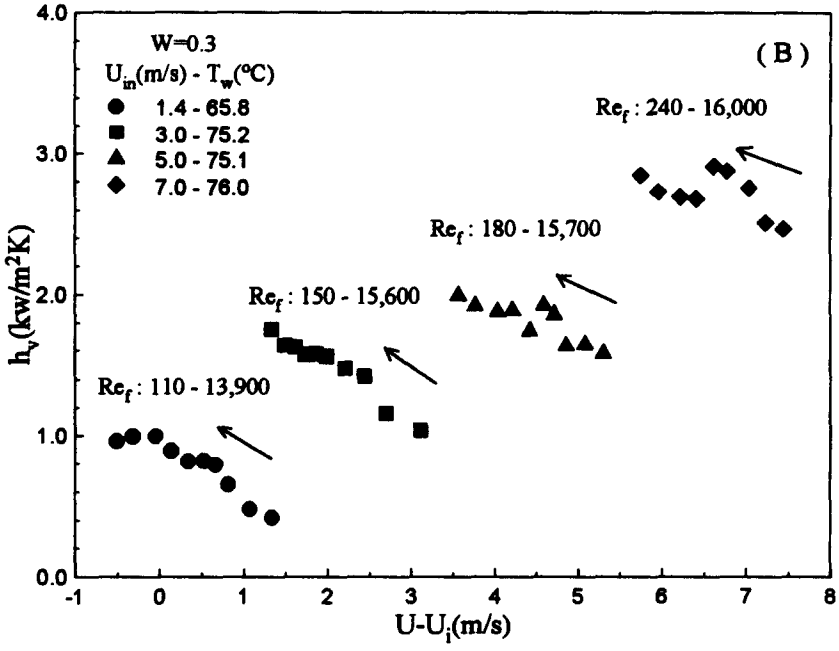

Fig. 4(b).

$$h_s = \frac{k_s \, \partial T/\partial y|_i}{T_b - T_i}. \qquad [10]$$

From the energy balance, the vapor-side heat transfer coefficient becomes

$$h_v = h_c + h_s. \qquad [11]$$

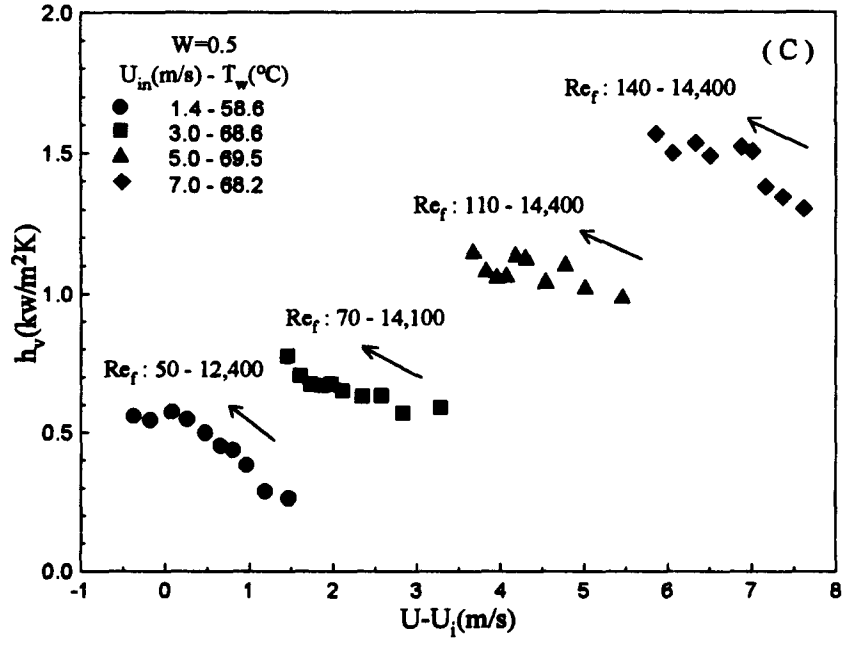

Fig. 4(c).

Figure 4. Vapor-side heat transfer coefficients with the vapor velocity relative to the moving condensate.

The condensing mass flux, m'', can be expressed by

$$m'' = \rho D\left(\frac{1}{W}\frac{\partial W}{\partial y}\right)_i = g\frac{W_b - W_i}{W_i} = g\frac{Y_i - Y_b}{1 - Y_i}, \quad [12]$$

where Y and W are steam- and air-mass fraction respectively, and g is the mass transfer coefficient.

Turbulent heat and mass transfer coefficients with negligible suction on a flat plate are commonly correlated in the form

$$g^o = C_m \mathrm{Re}_v^{0.8}\mathrm{Sc}^{1/3}\frac{\rho D}{x}, \quad [13]$$

$$h^o = \tilde{C}_s \mathrm{Re}_v^{0.8}\mathrm{Pr}^{1/3}\frac{k_s}{x}. \quad [14]$$

Since the boundary layer thicknesses are reduced due to the condensation, the following correction factors have to be implemented to account for the apparent suction effect (Kays and Crawford 1993)

$$g = \frac{\ln(1 + B_m)}{B_m} g^o; \quad B_m = \frac{Y_i - Y_b}{1 - Y_i} \quad [15]$$

$$h = \frac{\ln(1 + B_h)}{B_h} h^o; \quad B_h = \frac{m''/G}{\mathrm{St}}, \quad [16]$$

where B_h and B_m are the blowing parameters of heat and mass transfer corresponding to the friction blowing parameter at a transpired boundary layer.

Finally, the condensing heat transfer coefficient becomes

$$h_c = \frac{-h_{fv}}{T_b - T_i}\cdot\ln(1 + B_m)\cdot\frac{\rho D}{x}\cdot C_m \mathrm{Re}_v^{0.8}\mathrm{Sc}^{1/3}. \quad [17]$$

If the condensation conductivity is defined as

$$k_c = \frac{-h_{fv}}{T_b - T_i}\cdot\rho D\cdot\ln(1 + B_m), \quad [18]$$

[17] becomes

$$h_c = C_m \mathrm{Re}_v^{0.8}\mathrm{Sc}^{1/3}\frac{k_c}{x}. \quad [19]$$

Also, the sensible heat transfer coefficient including the suction effect becomes

$$h_s = C_s \mathrm{Re}_v^{0.8}\mathrm{Pr}^{1/3}\frac{k_s}{x}. \quad [20]$$

Since the form is very complex and the contribution to the total heat transfer rate is negligible, the correction factor of sensible heat transfer coefficient due to the suction is simply included in coefficient C_s. The vapor-side heat transfer coefficient, h_v, therefore, is expressed as the following equation from [11], [19] and [20]

$$h_v = C_m \mathrm{Re}_v^{0.8}\mathrm{Sc}^{1/3}\left\{k_c + \frac{C_s}{C_m}\cdot\left(\frac{\mathrm{Pr}}{\mathrm{Sc}}\right)^{1/3} k_s\right\}/x. \quad [21]$$

4.2. *Correlation of vapor-side heat transfer coefficients*

At first, C_m and C_s in [21] were obtained from the best fitting with the experimental data for the film Reynolds number less than 350. The number, 350, does not have a special meaning such as it is with the criterion dividing the surface of condensate film into smooth and wavy interface. It is very difficult to draw a definite line between smooth and wavy interface. The enhancement of vapor-side heat transfer coefficient due to the wavy interface increases smoothly with the increase of film Reynolds number. In order to analyze the enhancement due to the wavy interface, the data for film Reynolds number less than 350 were used as reference values with the negligible effect of the wavy interface. Figure 5 is the result of the best fitting. The coefficients, C_m and C_s/C_m, are 0.0283 and 2.5, respectively. Most data fitted within $\pm$ 10% error. The steam-mass fractions at the interface and the bulk fluid were obtained from the saturation temperature by assuming that the vapor mixture was saturated at the whole flow field. The vapor Reynolds numbers ranged from about 77,000 to 500,000.

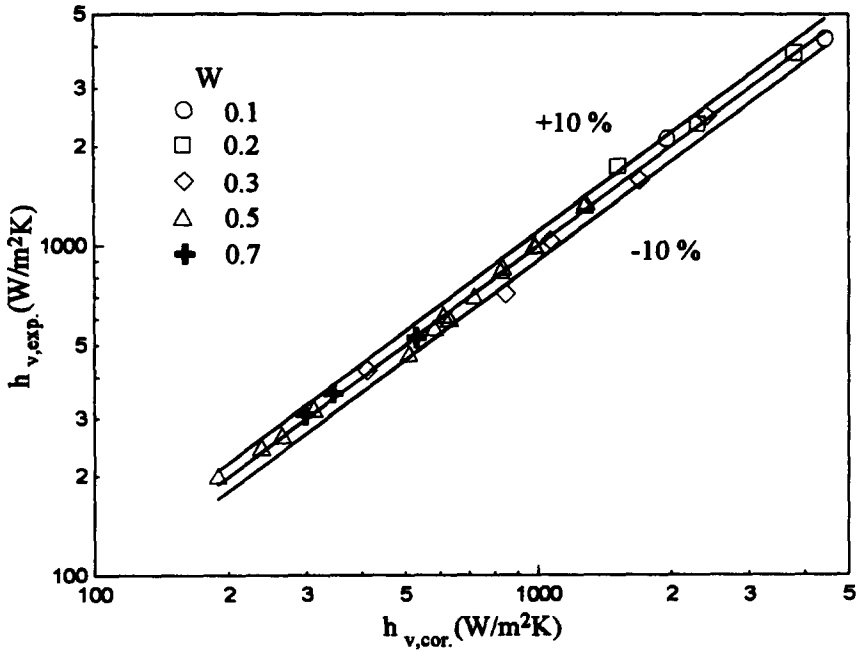

Figure 5. Comparison between the experimental data and the correlation [21] for $Re_f < 350$.

The coefficient, C_m, from the best fitting with the experimental data is 1.7% lower than 0.0288 of the result for a smooth flat plate, which was obtained from the local skin-friction coefficient for the Blasius relation using the Colburn analogy (Welty *et al.*, 1984). The sensible heat scaling coefficient, C_s, related to sensible heat transfer is 2.5 times the coefficient, C_m. The condensing heat scaling coefficient, $C_m = 0.0283$, matches the value, 0.0288, whereas the coefficient, C_s, is greater than the value for dry sensible heat transfer without condensation. One reason is that the multiplier considering the effect of suction is included in the sensible heat transfer scaling coefficient.

Peterson *et al.* (1993) correlated their experimental results for the condensation of a mixture of steam and non-condensable gas in vertical tubes as a form of the Dittus–Boelter equation. In their correlation the coefficients, C_m and C_s/C_m, were 0.0276 and 7.0 in the best curve-fitting. The reason C_m was greater by about 20% than 0.023 of the Dittus–Boelter correlation was attributed to the waviness of the condensate film. It was also suggested that the larger sensible heat scaling coefficient for a mixture condensation over that of a dry gas heat transfer, $C_s/C_m = 7$, was due to the increase of effective specific heat. If mist formation occurs in the vapor flow, the effective specific heat and thus the ratio $Pr/Sc = \rho C_p D/k_s$ increases substantially. Recently, Legay-Desesquelles and Prunet-Foch (1986) showed the enhancement of sensible heat transfer by using the turbulent boundary layer equation with considering mist formation. In, the present experiment the steam–air mixture was superheated from a few degrees to 25°C depending on the mass flow rate of steam. Therefore, the ratio of the sensible heat scaling coefficient to the condensing heat was supposed lower than the result of Peterson *et al.* (1993) with apparent mist formation.

Figure 6 shows the contribution of the sensible heat transfer to the total vapor-side heat transfer. While the condensation conductivity changes from about 0.8 to 9.6, the contribution of the sensible heat transfer decreases from about 9 to 1%.

Figure 7 shows a comparison between [21] and all data for the experiments of table 1. The film Reynolds number ranges from about 40 to 17,600. The arrow indicates the increase of condensate film Reynolds number in the figure. The comparison shows clearly the enhancement of heat transfer coefficient due to the rough and dynamic surface related to the film Reynolds number.

The enhanced heat transfer coefficient due to the wavy interface was correlated as

$$h_{v,w} = 0.0283 \cdot (1 + 1500 \cdot Re_f^{0.65} Re_v^{-1.1}) Re_v^{0.8} Sc^{1/3} \left\{ k_c + 2.5 \left(\frac{Pr}{Sc} \right)^{1/3} k_s \right\} / x. \quad [22]$$

Most of the experimental data fitted in [22] within $\pm 15\%$ error is shown in figure 8. In the present experimental range, the effects of the wavy interface on the enhancement of vapor-side heat transfer coefficient

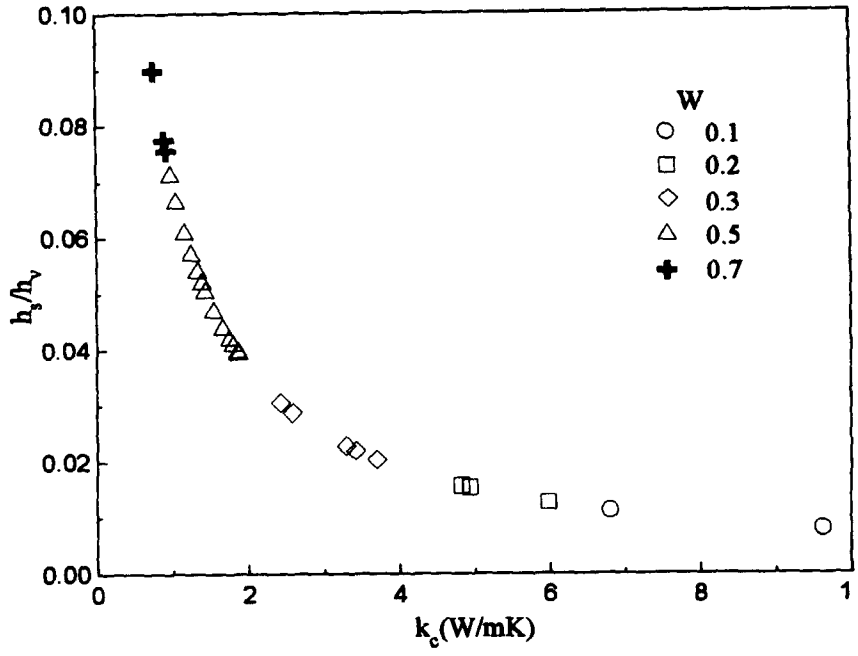

Figure 6. Contribution of sensible heat transfer to the total vapor-side heat transfer.

are well represented with condensate film Reynolds numbers and vapor Reynolds numbers between the parentheses in [22]. The enhancement depends linearly on the positive power to the film Reynolds number and increases with the increase of film Reynolds number. This is because the non-condensable gas layer is more strongly disturbed due to the enhanced roughness and waviness of the interface. Whereas the enhancement depends linearly on the negative power to the vapor Reynolds number and decreases with the increase of vapor Reynolds number. This means that the contribution of wavy interface to the enhancement decreases with the increase of the vapor Reynolds number. The larger the vapor Reynolds number is, the less

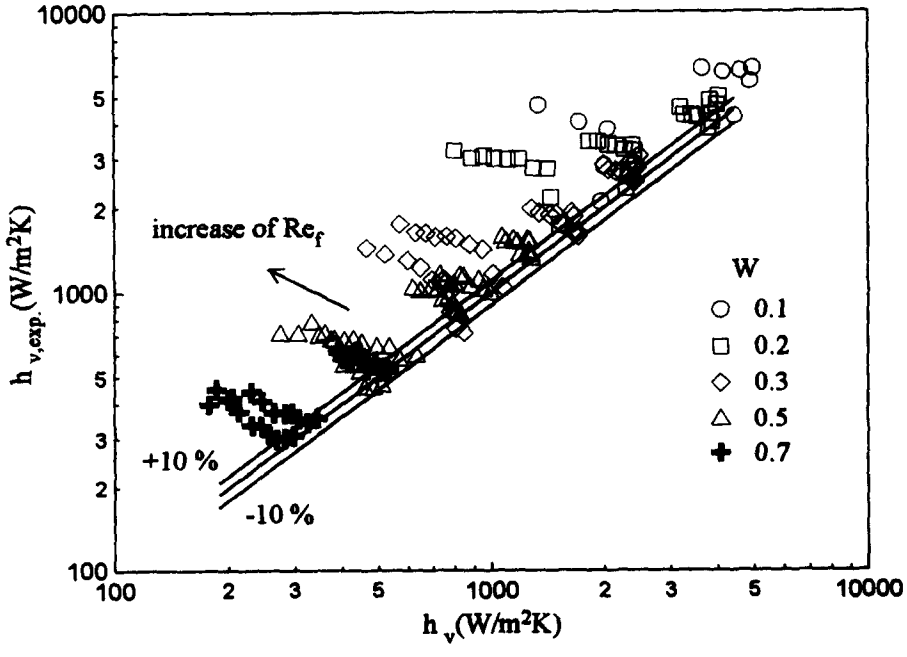

Figure 7. The enhanced vapor-side heat transfer coefficients due to the wavy interface corresponding to the film Reynolds number.

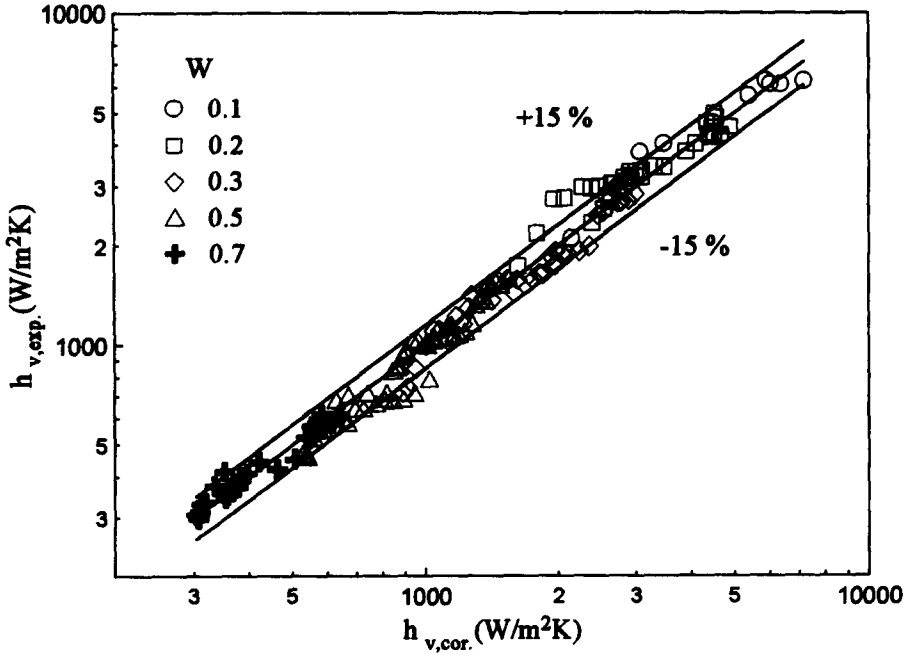

Figure 8. Comparison between the experimental data and the correlation [22].

is resistance of heat and mass transfer in the diffusion layer. That is, thermal resistance is greater for a low vapor Reynolds number than for a high vapor Reynolds number. Therefore, the enhancement effect due to the waviness is greater for the low vapor Reynolds number, although the waviness of vapor–condensate interface is the same.

5. CONCLUDING REMARKS

By using the analogy between heat and mass transfer, a correlation of the vapor-side heat transfer coefficients is proposed for the condensation of a steam–air mixture on a vertical surface. The correlation includes the effects of the wavy interface on the heat and mass transfer in the diffusion layer derived from a non-condensable gas. The vapor-side heat transfer coefficient was produced from the measured overall heat transfer coefficient across the condensate film and the diffusion layer by using an appropriate film-side heat transfer coefficient. The film-side heat transfer coefficient was estimated from a correlation of pure steam condensation on a vertical surface.

Under given conditions the vapor-side heat transfer coefficient increased greatly with the increase of the film Reynolds number. The enhancement was due to the wavy interface corresponding to the film Reynolds number. The experimental data were correlated separately according to the film Reynolds number. For a film Reynolds number less than 350, most of the data were well correlated as a function of vapor Reynolds number, air–mass fraction, Prandtl number, and Schmidt number within $\pm 10\%$. The ratio of the enhanced heat transfer coefficients for the wavy interface to those for a film Reynolds number less than 350 were correlated as a function of film Reynolds number and vapor Reynolds number. The film Reynolds numbers ranged from about 40 to 17,600 and the vapor Reynolds numbers from about 77,000 to 500,000. The air–mass fractions also ranged from 0.1 to 0.7. Most of the data were well fitted in the correlation within $\pm 15\%$. The enhancement increased with an increase of the film Reynolds number and decreased with an increase of the vapor Reynolds number for a given film Reynolds number.

Acknowledgements—This work was carried out with the support of KAERI (Korea Atomic Energy Research Institute) and AFERC (Advanced Fluids Engineering Research Center). The authors are grateful for the support.

REFERENCES

Al-Diwany, H. K. and Rose, J. W. (1973) Free convection film condensation of steam in the presence of non-condensing gases. *Int. J. Heat Mass Transfer* **16**, 1359–1369.

Asano, K., Nakano, Y. and Inaba, M. (1979) Forced convection film condensation of vapors in the presence of noncondensable gas on a small vertical flat plate. *J. of Chem. Engng of Japan* **12,** 196–202.

Bannwart, A. C. and Bontemps, A. (1990) Condensation of a vapour with incondensables: an improved gas phase film model accounting for the effect of mass transfer on film thickness. *Int. J. Heat Mass Transfer* **33,** 1465–1474.

Bean, H. S. (1971) *Fluid Meters: Their Theory and Application*, 6th ed. The American Society of Mechanical Engineers, New York.

Denny, V. E. and Jusionis, V. J. (1972) Effects of noncondensable gas and forced flow on laminar film condensation. *Int. J. Heat Mass Transfer* **15**, 315–326.

Hasanein, H. A., Kazini, M. S. and Golay, M. W. (1996) Forced convection in-tube steam condensation in the presence of noncondensable gases. *Int. J. Heat Mass Transfer* **39,** 2625–2639.

Huhtiniemi, J. K. and Corradini, M. L. (1993) Condensation in the presence of noncondensable gases. *Nucl. Eng. Design* **141**, 429–446.

Kang, H. C. and Kim, M. H. (1994) Effect of non-condensable gas and wavy interface on the condensation heat transfer in a nearly horizontal plate. *Nucl. Eng. Design* **149,** 313–321.

Karapantsios, T. D., Kostoglou, M. and Karabelas, A. J. (1995) Local condensation rates of steam–air mixtures in direct contact with a falling liquid film. *Int. J. Heat Mass Transfer* **38,** 779–794.

Kays, W. M. and Crawford, M. E. (1993) *Convective Heat and Mass Transfer*, 3rd ed. McGraw-Hill, New York.

Kim, M. H. and Corradini, M. L. (1990) Modeling of condensation heat transfer in a reactor containment. *Nucl. Eng. Design* **118,** 193–212.

Legay-Desesquelles, F. and Prunet-Foch, B. (1986) Heat and mass transfer with condensation in laminar and turbulent boundary layers along a flat plate. *Int. J. Heat Mass Transfer* **29,** 95–105.

Minkowycz, W. J. and Sparrow, E. M. (1966) Condensation heat transfer in the presence of noncondensables, interfacial resistance, superheating, variable properties and diffusion. *Int. J. Heat Mass Transfer* **9,** 1125–1144.

Nusselt, W. A. (1916) The surface condensation of water vapor. *Ziescrhift Ver. Deut. Ing.* **60,** 541–546.

Park, S. K. (1996) Effects of wavy interface on film condensation of steam–air mixture on a vertical surface. Ph.D. thesis, Pohang University of Science and Technology.

Park, S. K., Kim, M. H. and Yoo, K. J. (1996) Condensation of pure steam and steam–air mixture with surface waves of condensate film on a vertical wall. *Int. J. Multiphase Flow* **22,** 893–908.

Peterson, P. F., Schrock, V. E. and Kageyama, T. (1993) Diffusion layer theory for turbulent vapor condensation with noncondensable gases. *Trans. ASME* **115,** 998–1003.

Reid, R. C., Prausnitz, J. M. and Poling, B. E. (1987) *The Properties of Gases and Liquids*, 4th ed. McGraw-Hill, New York.

Rose, J. W. (1980) Approximate equations for forced convection condensation in the presence of a non-condensing gas on a flat plate and horizontal tube. *Int. J. Heat Mass Transfer* **23,** 539–546.

Schetz, J. A. (1993) *Boundary Layer Analysis*. Prentice-Hall, New York.

Slegers, L. and Seban, R. A. (1970) Laminar film condensation of steam containing small concentrations of air. *Int. J. Heat Mass Transfer* **13,** 1941–1947.

Sparrow, E. M., Minkowycz, W. J. and Saddy, M. (1967) Forced convection condensation in the presence of noncondensables and interfacial resistance. *Int. J. Heat Mass Transfer* **10,** 1829–1845.

Welty, J. R., Wicks, C. E. and Wilson, R. E. (1984) *Fundamentals of Momentum, Heat, and Mass Transfer*, 3rd ed. John Wiley & Sons, New York.

Yih, S. M. and Liu, J. L. (1983) Prediction of heat transfer in turbulent falling liquid films with or without interfacial shear. *AIChE J.* **29,** 903–909.